Article: 15646 / Vol. 569 No. 1 / Printed: Tuesday 12th February 2002 /

The Astrophysical Journal, 569:000–000, 2002 April 10

NEUTRINOS FROM EARLY-PHASE, PULSAR-DRIVEN SUPERNOVAE

J. H. Beall[1,2,3] and W. Bednarek[4]

Received 2001 August 6; accepted 2001 December 19

ABSTRACT

Q1 Neutron stars, just after their formation, are surrounded by expanding, dense, and very hot envelopes that
Q2 radiate thermal photons. Iron nuclei can be accelerated in the wind zones of such energetic pulsars to very high energies. These nuclei photodisintegrate, and their products lose energy efficiently in collisions with thermal photons and with the matter of the envelope, mainly via pion production. When the temperature of the radiation inside the envelope of the supernova drops below $\sim 3 \times 10^6$ K, these pions decay before losing energy and produce high-energy neutrinos. We estimate the flux of muon neutrinos emitted during such an early phase of the pulsar-supernova envelope interaction. We find that a 1 km^2 neutrino detector should be able to detect neutrinos above 1 TeV within about 1 yr after the explosion from a supernova in our Galaxy. This result holds if these pulsars are able to efficiently accelerate nuclei to energies $\sim 10^{20}$ eV, as postulated recently by some authors for models of Galactic acceleration of the extremely high energy cosmic rays (EHE CRs).

Subject heading: neutrinos — pulsars: general — radiation mechanisms: general — supernovae: general

1. INTRODUCTION

The production of neutrinos with different energies during supernova explosions has been discussed extensively during the last several years, mainly in the context of gamma-ray bursts (GRBs). For example, neutrinos with energies greater than 100 TeV can be produced in the interactions of protons accelerated by a fireball shock with GRB photons (e.g., Waxman & Bahcall 1997; Vietri 1998). TeV neutrinos can arise in interactions of protons with radiation when the fireball jet breaks through the stellar envelope (Meszaros & Waxman 2001). GeV neutrinos can also be produced in the interactions of protons with neutrons that can be present in the fireball models discussed by Derishev et al. (1999) and Meszaros & Rees (2000).

Of course, the acceleration of particles to high energies is also expected in the case of classical supernovae. Recently, Waxman & Loeb (2001) estimated the neutrino flux from a Type II supernova when the shock breaks out of its progenitor star. Berezinsky & Prilutsky (1978) and Protheroe, Bednarek, & Luo (1998) have estimated the flux of neutrinos produced by particles accelerated by the young pulsar during the early phase of the supernova explosion (see also the calculations for the Crab Nebula case in Bednarek & Protheroe 1997).

In this paper, we show that neutrinos can also be produced soon after the pulsar formation inside the supernova envelope, and that these neutrinos are detectable by current neutrino detectors. As shown by Blasi, Epstein, & Olinto (2000, hereafter BEO) and De Goubeia Dal Pino & Lazarian (2000), among others, particles can be accelerated to very high energies within the "plerion-like" region of a supernova shortly after the formation of the neutron star. We consider the scenario in which iron nuclei accelerated above the light cylinder of the pulsar interact: first, with the thermal radiation of the expanding supernova envelope, and later, with the matter of the envelope. Acceleration of hadrons in the pulsar wind zone has been discussed in the context of the production of high-energy cosmic rays since shortly after the discovery of pulsars (e.g., Gunn & Ostriker 1969; Karakuła, Osborne, & Wdowczyk 1974). For likely parameters of pulsars at birth, we predict that the flux of muon neutrinos can be observable by large-sized neutrino detectors during about 1 yr after supernova explosion.

2. THE PHYSICAL SCENARIO

We consider Type Ib/c supernovae, whose progenitors are Wolf-Rayet–type stars. Such stars evolve from massive stars with $M \geq 35\ M_\odot$, and create iron cores surrounded by relatively light envelopes of the order of a few solar masses. We use the models for the evolution of such stars and their explosions as published by Woosley et al. (1993). As an example, we concentrate on their model 60 WRA. The iron
Q4 core collapses to a very hot proto–neutron star that cools to the neutron star during about $t_{\rm NS} \approx 5$–10 s from the collapse (Burrows & Lattimer 1986; Wheeler et al. 2000). The rest of the mass of the pre-supernova (the envelope) is expelled with the velocity at the inner radius of the order of $v_1 = 3 \times 10^8$ cm s^{-1}. However, because of the density gradient, the outer parts of the envelope move faster. We approximate the velocities of matter in the envelope by the profile

$$v(R) = v_1 (R/R_1)^b \,, \tag{1}$$

where the parameter $b = 0.5$ is obtained from an approximation of the velocity profile in the expanding envelope shown in Figure 9 in Woosley et al. (1993), and we use $R_1 = 3 \times 10^8$ cm as the inner radius of the envelope at the moment of explosion. The density of matter in the envelope just before the collapse of the iron core can be approximated

[1] E. O. Hulburt Center for Space Research, Naval Research Laboratory, Washington, DC 20375.
[2] Center for Earth Observing and Space Research, School for Computational Sciences, George Mason University, Fairfax, VA 22030.
[3] St. John's College, P.O. Box 2800, Annapolis, MD 21404.
[4] Department of Experimental Physics, University of ódź, ul. Pomorska 149/153, PL 90-236 ódź, Poland.

by the profile

$$n(R) = n_1(R/R_1)^{-a}\,, \tag{2}$$

where the density at R_1 is $n_1 = 1.2 \times 10^{31}$ cm^{-3}, and the parameter $a = 2.4$ is obtained from Figure 1 in Khokhlov et al. (1999) by interpolation of the profiles for the radius and density versus the mass of the pre–supernova star (see also Fig. 3*c* in Woosley et al. 1993). The initial column density decreases with time, t, as a result of the expansion of the envelope according to

$$\rho(t) = \int_{R_1}^{R_2} n(R)\left[\frac{R}{R + v(R)t}\right]^2 dR\,, \tag{3}$$

where $R_2 = 3 \times 10^{10}$ cm is the outer radius of the envelope at the moment of explosion, and $v(R)$ and $n(R)$ are given by equations (1) and (2), respectively. Just after the collapse of the iron core, the temperature at the bottom of the envelope is $T_0 \approx 3 \times 10^9$ K at R_1 (see Fig. 8 in Woosley et al. 1993). Therefore, the volume above the pulsar and below the
Q5 expanding envelope is filled with thermal radiation that is not able to escape because of the high optical depth of the
Q6 envelope. We apply the formula that the temperature of this radiation drops with time during the expansion of the envelope according to

$$T(t) = T_0\left(\frac{R_1}{R_1 + v_1(t_{\rm NS} + t)}\right)^{3/4}. \tag{4}$$

At the moment of the neutron star's formation (after $\sim$10 s), the temperature in the region below the envelope already drops to $\sim 5 \times 10^8$ K.

We assume that at this early age, the pulsar loses energy only via electromagnetic radiation. Therefore, its period changes according to the formula $P_{\rm ms}^2(t) = 1.04 \times 10^{-9} t B_{12}^2 + P_{0,\rm ms}^2$, where $P_{0,\rm ms}$ $P_{\rm ms}$ are the initial and present periods of the pulsar (in milliseconds), and B_{12} is the pulsar surface magnetic field in units 10^{12} G. Note that after about 1 yr, the pulsar may also efficiently lose energy on emission of gravitational radiation because of the r-mode instabilities
Q7 that are excited in cooling neutron stars (e.g., Andersson 1998; Lindblom, Owen, & Morsink 1998). During this time, it is likely that the pulsar period changes, suddenly reaching the value $\sim$10–15 ms at about 1 yr after formation.

During the first year after explosion, the rate of rotational energy loss by the pulsar is too low to influence the initial expansion velocity of the envelope (Ostriker & Gunn 1971), assuming that the pulsar has been born with parameters
Q8 characteristic ofthe classical radio pulsars (e.g., the Crab pulsar). Only pulsars with periods of the order of a few milliseconds and superstrong magnetic fields (magnetars) can significantly accelerate the envelope at short time intervals after the explosion.

In § 3, we consider the acceleration of the iron nuclei in the pulsar magnetosphere above the light cylinder and below the expanding envelope, adopting the aforementioned model for the formation of the pulsar and the expansion of the supernova envelope. During the first year after the explosion, when the supernova envelope is very dense, the nuclei interact with the dense radiation field below the envelope and the matter of the envelope. Our aim is to find out if the acceleration and radiation processes inside the expanding envelope can produce an observable flux of neutrinos during the early phase of a supernova explosion.

3. ACCELERATION OF IRON NUCLEI

Observations of young plerions (e.g., the Crab Nebula) indicate that most of the rotational energy of the pulsar is converted into relativistic particles in the pulsar wind (e.g., Rees & Gunn 1974; Kennel & Coroniti 1984). However, the details of how the wind dissipates the pulsar rotational energy remain a topic of current research.

It has been argued that an ideal, ultrarelativistic MHD wind is not able to convert the Poynting flux into particles (see, e.g., Chiueh, Li, & Begelman 1998; Bogovalov & Tsinganos 1999). This difficulty could be overcome by means of the rapid expansion of the wind in a magnetic nozzle (Chiueh et al. 1998) or by nonidealized MHD effects in a two-fluid plasma (Melatos & Melrose 1996). Recent analysis of the propagation of an MHD wind (Contopoulos & Kazanas 2002), based on an exact solution of the axisymmetric magnetosphere (Contopoulos, Kazanas, & Fendt 1999), shows that the Lorentz factor of an outflowing plasma increases linearly with the distance from the light cylinder up to the moment when the flow collimates drastically toward the direction of the axis of symmetry.

Another possible explanation for the conversion of the Poynting flux into particle energy is that particles are accelerated in the reconnection of oppositely directed magnetic fields in the wind (Michel 1982; Coroniti 1990). Investigations of this process by Lyubarsky & Kirk (2001) show that since the wind accelerates in the course of reconnection, the conversion of Poynting flux to particle energy must occur on longer timescales, and that the process becomes inefficient for pulsars with Crab-like parameters, although it is still efficient for millisecond pulsars. In addition, the type of
Q9 particles thatdominate in the wind is not well determined. It is plausible that iron nuclei, stripped from the hot surface of a young neutron star, can play an essential role (Ruderman 1981; Arons 1983). For example, such ions might resonantly accelerate positrons and electrons to the energies necessary to explain the TeV γ-ray emission from the Crab Nebula (Gallant & Arons 1994).

In the present study, we follow the work by BEO and assume that the magnetic energy in the pulsar's wind zone accelerates iron nuclei via the so-called "magnetic slingshot" mechanism (Gunn & Ostriker 1969). Since this acceleration occurs very early (i.e., during the first month after supernova explosion), the nuclei photodisintegrate in collisions with thermal photons and lose energy on inelastic collisions as they propagate in the radiation field below the supernova envelope, but not during the acceleration process. The energies that the iron nuclei can reach in the wind zone depend on the pulsar parameters, so that

$$E_{\rm Fe} = \frac{B^2(r_{\rm LC})}{8\pi n_{\rm GJ}(r_{\rm LC})} \approx 1.8 \times 10^{11} B_{12} P_{\rm ms}^{-2}\ {\rm GeV}\,, \tag{5}$$

where $r_{\rm LC} = cP/2\pi$ is the light cylinder radius, and $n_{\rm GJ} = B(r_{\rm LC})/(2eZcP)$ is the Goldreich & Julian (1969) density at the light cylinder. As an example, we show the temperature of the radiation field below the envelope of the supernova and the energies of accelerated iron nuclei as a function of time in Figure 1, for the case of two pulsars with parameters $B_{12} = 4$, $P_{\rm ms} = 3$, and $B_{12} = 100$, $P_{\rm ms} = 10$. Note that in the case of the first pulsar, its period does not change, and consequently, the energies of the iron nuclei do not change significantly during the first $\sim$1 yr after the explosion, contrary to the case for the second pulsar.

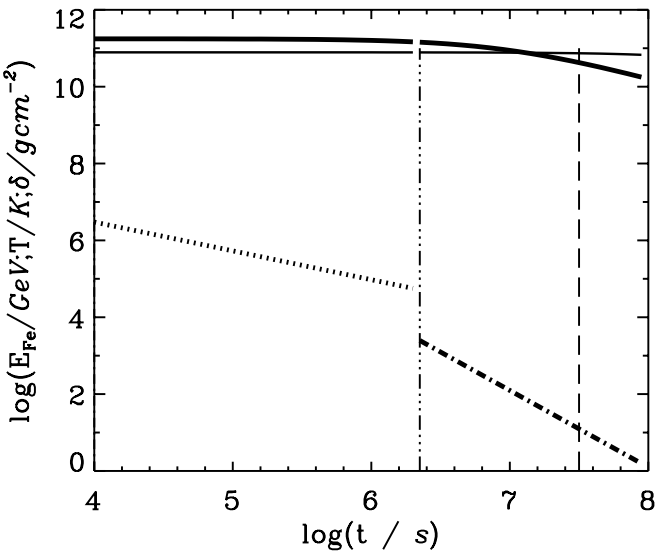

FIG. 1.—Dependence of the maximum energies of accelerated iron nuclei, the temperature of the thermal radiation in the acceleration region (*dotted curve*), and the column density of matter in the envelope (*thick dot-dashed curve*), shown as a function of time that is measured from the supernova explosion. Iron nuclei are accelerated by the pulsars with initial parameters $B_{12} = 4$, $P_{\rm ms} = 3$ (*thin solid curve*) and $B_{12} = 100$, $P_{\rm ms} = 10$ (*thick solid curve*). The vertical lines mark the times after which the envelope becomes transparent to thermal radiation (*dot-dot-dot-dashed line*), and at which the envelope becomes transparent to hadronic collisions, and the parameters of the neutron star may change drastically because of energy losses through gravitational radiation (*long-dashed line*).

We obtain the spectrum of iron nuclei accelerated in the pulsar wind zone close to its light cylinder by following the general prescription given by BEO. In this simple model, all nuclei are accelerated to the energy, $E_{\rm Fe}$, and their number is part of the Goldreich & Julian density, $n = \xi n_{\rm GJ}$. However, contrary to that work, we assume that the pulsar with specific parameters (B_{12} and $P_{\rm ms}$) injects particles within some range of energies, because of the fact that the magnetic field at different parts of the light cylinder radius (and so the Poynting flux) is different. The magnetic field strength at the height h, measured from the plane containing the pulsar and perpendicular to the light cylinder radius, can be expressed by $B(r) \approx B(r_{\rm LC})\cos\alpha$, where $\cos\alpha = r_{\rm LC}/(r_{\rm LC}^2 + h^2)^{1/2}$. Therefore, the density of particles at the light cylinder $n(h) = n_{\rm GJ}\cos^3\alpha$, and their energies, $E = E_{\rm Fe}\cos^3\alpha$, depend on h. We calculate the number of particles injected at the height h per unit time from $dN/dt = 2\pi r_{\rm LC} c n(h) dh$. Using the above formulae, we replace dh with dE and obtain the differential spectrum of iron nuclei injected by the pulsar at the fixed age of the pulsar, t:

$$\frac{dN}{dE\,dt} = \frac{2\pi c\xi r_{\rm LC}^2 n_{\rm GJ}(r_{\rm LC})(E_{\rm Fe}E^2)^{-1/3}}{3\left[(E_{\rm Fe}/E)^{2/3} - 1\right]^{1/2}} \cong \frac{3\times 10^{30}\eta(B_{12}P_{\rm ms}^{-2}E^{-1})^{2/3}}{\left[(E_{\rm Fe}/E)^{2/3} - 1\right]^{1/2}}\ \frac{\rm Fe}{\rm s\ GeV}\ . \qquad (6)$$

Note that our parameter ξ has similar meaning to the parameter ξ introduced by BEO. Because of the shape of the spectrum of iron nuclei $\propto E^{-1/3}$ (eq. [6]), in our model also most of the iron nuclei reaches the energies from the highest energy part of this spectrum at $E_{\rm Fe}$, given by equation (5).

In this paper we discuss only the consequences of acceleration of iron nuclei at a relatively early phase after the supernova explosion (i.e., up to about 1 yr from pulsar formation). During this time the radiation field inside the expanding supernova envelope, and thereafter the column density of the envelope, are high enough to provide a target for relativistic nuclei. As we have already noted, the period of the neutron star can be significantly influenced by gravitational energy losses after about 1 yr from the time of the explosion, when the neutron star cools enough.

4. PRODUCTION OF NEUTRINOS

We consider the acceleration of nuclei in the pulsar wind when the pulsar is immersed in the dense thermal radiation filling the cavity below expending supernova envelope. Since the supernova envelope is opaque for nuclei and radiation only during about 1 yr after explosion, we are interested in processes that occur during this very early phase of the pulsar–supernova remnant interaction.

Accelerated nuclei move in the pulsar wind almost at rest in the wind reference frame (BEO). Therefore, they do not lose significant energy by synchrotron emission. As we have noted, however, these nuclei will interact with the strong thermal radiation field in the supernova cavity, suffering multiple photodisintegration of nucleons. Since the mean free paths for photodisintegration of iron (and lighter) nuclei are significantly shorter than for their energy losses on $e^{\pm}$ pair and pion production (e.g., Karakuła & Tkaczyk 1993), the nuclei suffer complete disintegration onto nucleons before significant energy losses. For plausible parameters of the pulsar and the acceleration region, these secondary nucleons lose energy mainly via pion production. The pions then decay into high-energy neutrinos if their decay distance scale $\lambda_\pi \approx 780\gamma_\pi$ cm is shorter than their characteristic energy loss mean free path. The Lorentz factors of pions, γ_π, are comparable to the Lorentz factors of their parent protons, so they move similarly in the pulsar wind, and their synchrotron losses should not dominate over their inverse Compton losses (ICS) in the thermal radiation. Pions lose energy on ICS process mainly in the Klein-Nishina (KN) regime, but not very far from the border with the Thomson regime. Therefore, we can estimate the ICS losses of pions in the KN regime by

$$P_{\rm KN}^{\rm ICS} \approx 4/3\pi\sigma_{\rm T} U_{\rm rad}(m_e/m_\pi)^2\gamma_{\rm KN/T}^2\ , \qquad (7)$$

where $\sigma_{\rm T}$ is the Thomson cross section, $U_{\rm rad}$ is the energy density of radiation, m_e, m_π are the masses of electron and pion, and $\gamma_{\rm KN/T} \approx 5\times 10^{11}/T$ is the Lorentz factor at the transition between the KN and T regimes. We estimate the mean free path for pion energy losses via ICS,

$$\lambda_{\rm ICS} \approx m_\pi\gamma_\pi/P_{\rm KN}^{\rm ICS} \approx 10^{16}\gamma_\pi/T^2\ {\rm cm}\ , \qquad (8)$$

where $\lambda_{\rm ICS}$ is comparable to the pion decay distance, λ_π, only for temperatures of radiation $T \le 3\times 10^6$ K. Thus, pions decay before significant energy losses only if this condition is fulfilled.

The temperature of the radiation inside the envelope drops to $T \le 3\times 10^6$ K at about $t_{\rm dec} \sim 10^4$ s after the supernova explosion (see eq. [4]). At that moment, nucleons from disintegration of nuclei cool in collisions with thermal radiation mainly by pion production. However, when the optical

depth through the expanding envelope drops below $\sim 10^3$, the radiation is not further confined in the region below the envelope, and its temperature drops rapidly. Based on equations (1), (2), and (3), we have found that this happens at the time $t_{\rm conf} \sim 2 \times 10^6$ s after the explosion (see Fig. 1, *thin dot-dot-dot-dashed line*). Therefore, we conclude that nucleons are able to cool efficiently in the thermal radiation and produce pions, which then decay into muon neutrinos, but only from $t_{\rm dec} \approx 10^4$ s up to $t_{\rm conf} \approx 2 \times 10^6$ s after the explosion. At later times, the relativistic iron nuclei do not disintegrate in the radiation field but interact directly with the matter of the envelope, whose density is already low enough so that pions produced by that interaction are able to decay into neutrinos and muons.

We now compute the differential spectra of muon neutrinos produced in the interaction of nuclei (1) with the radiation field below the envelope during the period 1×10^4–2×10^6 s after the supernova explosion, and (2) with the matter of the envelope during the period from 2×10^6 to 3×10^7s after the explosion, assuming that the nucleons cool to the lowest energies allowed by the column densities of photons and matter, respectively. In this calculation, we assume that pions are produced in N-γ collisions with the Lorentz factors comparable to their parent nucleons. In the case of iron-matter (Fe-M) interactions, we apply the pion multiplicities given in Orth & Buffington (1976). As an example, we show the results of these calculations (Fig. 2) for three pulsars with initial parameters: $P_{\rm ms} = 3$ and $B_{12} = 4$ (model I; *dashed histogram*), $P_{\rm ms} = 20$ and $B_{12} = 4$ (model II; *dotted histogram*), and $P_{\rm ms} = 10$ and $B_{12} = 100$ (model III; *solid histogram*). The iron nuclei accelerated by pulsars according to models I and III fulfill the condition $P_{\rm ms} \approx 4(B/10^{13}\ {\rm G})^{1/2}$ (given by BEO), which allows them to reach energies 10^{20} eV. Note that even in the case of the model III, the energy losses of the pulsar during the first year after its formation do not overcome the total kinetic energy of the envelope. Therefore, the envelope is not accelerated. Model II describes the pulsar with the presumable parameters of the Crab pulsar at birth. The periods of pulsars in models I and II do not change drastically during the first year after the supernova explosion. However, the period of the pulsar in model III changes by a factor of $\sim$3, which causes the change in energy of the iron nuclei by about an order of magnitude during one year after explosion.

The numbers of neutrinos produced in these two processes do differ significantly, because of the fact that pion multiplicities in N-γ and Fe-M interactions are different. Therefore, the neutrino fluxes from Fe-M interactions are up to an order of magnitude higher than the neutrino fluxes from N-γ interactions. Note also that the column density of the envelope after $\sim 2 \times 10^6$ s drops rapidly with time, and only nuclei injected earlier than $\sim 10^7$ s can undergo multiple interactions with matter.

Since in model III the energies of accelerated iron nuclei significantly change during the first year, it is interesting to investigate how the spectrum of neutrinos changes with time in this case. In Figure 3 we show the spectra of neutrinos for the model III produced at different ranges of time after pulsar formation. The neutrino spectra have comparable intensities before $\sim 2 \times 10^6$ s after explosion (during N-γ production phase) with the cutoffs at this same energy (the pulsar periodsdo not change significantly during this time; see Fig. 1). However, the location of the lower energy break in the neutrino spectra shifts with time to higher energies, since it is determined by the temperature of radiation, which drops with time. The highest fluxes of neutrinos are expected at $\sim 2 \times 10^6$–10^7 s after explosion during the interaction of iron nuclei with the matter of the supernova envelope. At later times (10^7–3×10^7 s), the neutrino flux drops significantly, because particles, already accelerated to lower

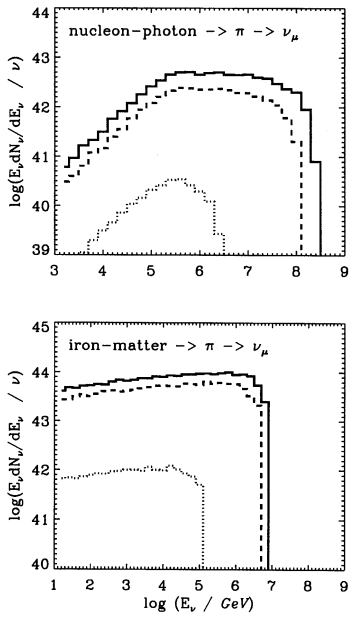

FIG. 2.—Spectra of muon neutrinos and antineutrinos produced in interactions of nucleons from photodisintegration of iron nuclei with the thermal radiation field inside the supernova envelope ($N - \gamma \rightarrow \pi \rightarrow \nu_\mu$), and from interactions of iron nuclei with the matter of the envelope (Fe − M $\rightarrow \pi \rightarrow \nu_\mu$). The density factor is $\xi = 1$, and the initial periods and the surface magnetic fields of the pulsars are: $P_{\rm ms} = 10$ and $B_{12} = 100$ (*solid histograms*), $P_{\rm ms} = 3$ and $B_{12} = 4$ (*dashed*), and $P_{\rm ms} = 20$ and $B_{12} = 4$ (*dotted*).

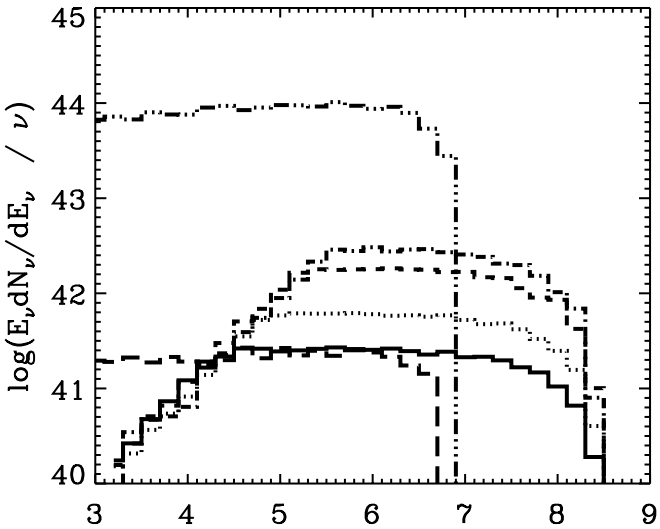

FIG. 3.—Spectra of muon neutrinos and antineutrinos produced by the pulsar with the parameters of model III ($B_{12} = 100$ and $P_{\rm ms} = 10$) at different range of time measured from the pulsar formation: $\Delta t = 10^4 - 10^5$ s (*solid histogram*), 10^5–3×10^5 s (*dotted*), 3×10^5–10^6 s (*dashed*), 10^6–2×10^6 s (*dot-dashed*), 2×10^6–10^7 s (*dot-dot-dashed*), and 10^7–3×10^7 s (*long-dashed*).

energies, are not completely cooled in collisions with the matter of the envelope (see Fig. 1).

Just after the collapse of the iron core, the column density of matter is high enough to absorb the neutrinos with energies above $\sim$0.1 GeV. However, the column density drops quickly with time ($\propto t^{-2}$, see eq. [4]), and the cross section for neutrino interaction with matter increases with energy $\propto E_\nu$ and $\propto E_\nu^{0.4}$ below and above $E_\nu \sim 1$ TeV, respectively (e.g., Hill 1997). Therefore, the optical depth becomes less than 1 at times $\sim 10^4$ s even for the highest energy neutrinos produced.

5. DISCUSSION AND CONCLUSION

For a supernova inside our Galaxy at a distance, $D = 10$ kpc, we estimate the expected flux of muon neutrinos produced (in nucleon-photon interactions during 1×10^4–2×10^6 s after the explosion and produced in nuclei-matter collisions during 2×10^6–3×10^7 s after the explosion) by integrating the neutrino spectra shown in Figure 2. The likelihood of detecting these neutrinos by a detector with a surface area of 1 km^2 can be obtained using the probability of neutrino detection given by Gaisser & Grillo (1987). The results of our calculations, for the surface magnetic fields and initial periods of pulsars specified by models I, II, and III, and the density factor $\xi = 1$, are shown in Table 1 for the case of neutrinos arriving from directions close to the horizon, i.e., not absorbed by the Earth (H), and for neutrinos that arrive moving upward from the nadir direction and are partially absorbed (N) (for absorption coefficients see Gandhi 2000). We investigated in more detail model III, for which the time-dependent neutrino spectra are calculated (see Fig. 3). The expected time-dependent number of neutrinos detected by a 1 km^2 detector,in this case for the horizontal and nadir directions, is: 1.1×10^3 (H) and 250 (N) (at $\Delta t = 10^4$–10^5 s), 2.7×10^3 and 590 (10^5–3×10^5 s), 7.9×10^3 and 1.7×10^3 (3×10^5–10^6 s), 1.2×10^4 and 2.5×10^3 (10^6–2×10^6 s), 1.8×10^5 and 6.4×10^4 (2×10^6–10^7 s), and 400 and 150 (10^7–3×10^7 s). The highest detection rates of neutrinos are expected during about 1–2 months after supernova explosion from the phase of particle interaction with the matter of the envelope.

If extremely high energy cosmic rays (EHE CRs) are produced by pulsars within our Galaxy, then the observed flux of particles allows us to constrain some free parameters of the considered model. By comparing the observed flux of cosmic rays at $\sim 10^{20}$ eV with model estimations of the flux of iron nuclei, BEO finds that the following condition should be fulfilled: $\xi \epsilon Q / \tau_2 R_1^2 B_{13} \approx 4 \times 10^{-6}$, where ξ is the efficiency for accelerating particles defined similarly as in our paper, ϵ is the fraction of pulsars thathave the parameters required for particle acceleration to 10^{20} eV, Q is the trapping factor of particles within the Galactic halo, $\tau = 100\tau_2$ yr is the rate of neutron star production, $R = 10R_1$ kpc is the radius of the Galactic halo, and $B_{13} = 0.1B_{12}$ is the pulsar surface magnetic field. For plausible parameters $\tau_2 = 1$, $R_1 = 3$ (required by the condition of isotropization of EHE CRs), $Q \sim 1$ (see recent calculations of the propagation of hadrons within the Galaxy and halo by Alvarez-Muniz, Engel, & Stanev 2001; Bednarek, Giller, & Zielińska 2001; and O'Neill, Olinto & Blasi 2001), and the rate of formation of neutron stars with required parameters equal to about 10% ($\epsilon = 0.1$), we obtain the limit on the particle acceleration efficiency $\xi \approx 10^{-4}$ for model I, and $\xi \approx 4 \times 10^{-3}$ for model III. These simple estimations, combined with the results of our calculations of the numbers of expected neutrinos, presented in Table 1, show that some neutrinos might be observed in the 1 km^2 detector in the case of the pulsar described by model I and a few hundred neutrinos in the case of model III. However, because of the steepness of the cosmic ray spectrum, such limits should be less restrictive for the pulsars accelerating particles to lower energies (less than 10^{20} eV). We conclude that the detection of neutrinos from early phase of supernovae (or lack thereof) will put constraints on the recent models of extremely high energy cosmic ray production in supernova explosion with formation of very energetic pulsars (BEO; De Goubeia Dal Pino & Lazarian 2000).

It is clear from Table 1 that neutrinos from a Crab-type pulsar located at the distance of $\sim$2 kpc (see model II) might be observable by the 1 km^2 neutrino detector during the first year after pulsar formation if the particle acceleration efficiency is $\xi > 3 \times 10^{-3}$. Therefore, it is likely that a recent explosion of a supernova at a distance similar to that of historical supernovae can also constrain the parameter ξ.

If the model considered here obtains for extragalactic supernovae, then the whole population of pulsars created in the universe should contribute to the extragalactic neutrino background. Such a neutrino flux might be detectable, since extragalactic neutrinos from pulsars could be expected to be seen during their early neutrino-producing phase. This interesting problem is considered in another paper (Bednarek 2001), in which we estimate the extragalactic neutrino background from the population of pulsars with parameters similar to those of classical radio pulsars formed in the universe.

In fact, neutrinos can also be produced in later stages of supernova explosions, when the capturing of relativistic particles by the supernova envelope is efficient. Such scenarios have been considered in the case of proton acceleration in the pulsar's wind zone (Berezinsky & Prilutsky 1978), and in the case of hadron acceleration in the pulsar's inner magnetosphere (Bednarek & Protheroe 2001; Protheroe, Bednarek, & Luo 1998). However, such a production of neutrinos is less certain, since it is expected that neutron stars can lose energy very efficiently via gravitational waves at about 1 yr after the explosion as a result of the *r*-mode instabilities. It has been argued that *r*-mode instabilities are

TABLE 1

EXPECTED NUMBER OF DETECTED ν_μ

Interaction	$P_{ms} = 3, B_{12} = 4$	$P_{ms} = 20, B_{12} = 4$	$P_{ms} = 10, B_{12} = 100$
N-$\gamma \rightarrow \nu_\mu$ (H)	8.4×10^3	2.6	2.4×10^4
Fe-M$\rightarrow \nu_\mu$ (H)	8.7×10^4	11.3	1.8×10^5
N-$\gamma \rightarrow \nu_\mu$ (N)	2×10^3	1.1	5.1×10^3
Fe-M$\rightarrow \nu_\mu$ (N)	3.4×10^4	8.6	6.4×10^4

Article: 15646 / Vol. 569 No. 1 / Printed: Tuesday 12th February 2002 /

not excited in the neutron stars with the surface magnetic fields typical for magnetars, i.e., $B \gg 10^{13}$ G (Rezzolla, Q21 Lamb, & Shapiro 2000). Detection of neutrinos at these later times might militate against the *r*-mode instabilities as a means of the production of gravitational radiation. This in turn could have implications for the likelihood of detection of gravitational radiation associated with neutron star production. On the other hand, a sharp cutoff in the detected neutrino flux from a supernova could corroborate the existence of *r*-mode instabilities and lend credence to the possibility of gravity wave generation and detection. Such a detection is of preeminent theoretical interest.

We are grateful to the anonymous referee for comments and suggestions that have improved this paper. W. B. thanks the School for Computational Sciences (SCS) at George Mason University at Fairfax, VA, for hospitality during his visit. The research of W. B. was supported by the Polish KBN grant 5P03D 025 21.

REFERENCES

Alvarez-Muniz, J., Engel, R., & Stanev, T. 2001, in Proc. 27th Int. Cosmic-Ray Conf. (Hamburg), 1972
Andersson, N. 1998, ApJ, 502, 708
Arons, J. 1983, ApJ, 266, 215
Bednarek, W. 2001, A&A, 378, L49
Bednarek, W., Giller, M., & Zielińska, M. 2001, in Proc. 27th Int. Cosmic-Ray Conf. (Hamburg), 1976
Bednarek, W., & Protheroe, R. J. 1997, Phys. Rev. Lett., 79, 2616
Q22 ———. 2001, Astropart. Phys., in press
Q23 Berezinsky, V. S., & Prilutsky, O. F. 1978, A&A, 66, 325
Blasi, P., Epstein, R. I., & Olinto, A. V. 2000, ApJ, 533, L123 (BEO)
Bogovalov, S. V., & Tsinganos, K. 1999, MNRAS, 305, 211
Burrows, A., & Lattimer, J. M. 1986, ApJ, 307, 178
Chiueh, T., Li, Y.-Z., & Begelman, M. C. 1998, ApJ, 505, 835
Q24 Contopoulos, I., & Kazanas, D. 2002, ApJ, 566, 336
Contopoulos, I., Kazanas, D., & Fendt, C. 1999, ApJ, 511, 351
Coroniti, F. V. 1990, ApJ, 349, 538
De Goubeia Dal Pino, E. M., & Lazarian, A. 2000, ApJ, 536, L31
Derishev, E. V., Kocharovsky, V. V., & Kocharovsky, Vl. V. 1999, ApJ, 521, 640
Q25 Gaisser, T. K., & Grillo, A. F. 1987, Phys. Rev. D, 39, 1481
Gallant, Y. A., & Arons, J. 1994, ApJ, 435, 230
Q26 Gandhi, R. 2000, Nucl. Phys. Suppl., 91, 453
Goldreich, P., & Julian, W. H. 1969, ApJ, 157, 869
Gunn, J., & Ostriker, J. 1969, Phys. Rev. Lett., 22, 728
Hill, G. C. 1997, Astropart. Phys., 6, 215
Q27 Karakuła, S., Osborne, J. L., & Wdowczyk, J. 1974, J. Phys. A, 7, 437
Karakuła, S., & Tkaczyk, W. 1993, Astropart. Phys., 1, 229
Kennel, C. F., & Coroniti, F. V. 1984, ApJ, 283, 694
Khokhlov, A. M., et al. 1999, ApJ, 524, L107
Lindblom, L., Owen, B. J., & Morsink, S. M. 1998, Phys. Rev. Lett., 80, 4843
Lyubarsky, Y., & Kirk, J. G. 2001, ApJ, 547, 437
Melatos, A., & Melrose, D. B. 1996, MNRAS, 279, 1168
Meszaros, P., & Rees, M. J. 2000, ApJ, 541, L5
Meszaros, P., & Waxman, E. 2001, Phys. Rev. Lett., 87, 1102
Michel, F. C. 1982, Rev. Mod. Phys., 54, 1
O'Neill, S., Olinto, A., & Blasi, P. 2001, in Proc. 27th Int. Cosmic-Ray Conf. (Hamburg), 1999
Orth, C. D., & Buffington, A. 1976, ApJ, 206, 312
Ostriker, J. P., & Gunn, J. E. 1971, ApJ, 164, L95
Protheroe, R. J., Bednarek, W., & Luo, Q. 1998, Astropart. Phys., 9, 1
Rees, M. J., & Gunn, J. E. 1974, MNRAS, 167, 1
Rezzolla, L., Lamb, F. K., & Shapiro, S. L. 2000, ApJ, 531, L139
Q28 Ruderman, M. 1981, in Pulsars (Dordrecht: Reidel), 87
Vietri, M. 1998, Phys. Rev. Lett., 80, 3690
Waxman, E., & Bahcall, J. 1997, Phys. Rev. Lett., 78, 2292
Waxman, E., & Loeb, A. 2001, Phys. Rev. Lett., 87, 1101
Wheeler, J. C., Yi, I., Höflich, P., & Wang, L. 2000, ApJ, 537, 810
Woosley, S. E., Langer, N., & Weaver, T. A. 1993, ApJ, 411, 823

Q1 au: Your article has been edited for grammar, consistency, and to conform to ApJ journal style (see Instructions to Authors). To expedite publication, we generally do not query every routine grammatical and style change made to a manuscript, although all substantive changes have been noted. Please review the article carefully. Note that we may be unable to make changes that conflict with journal style, obscure meaning, or create grammatical or other problems. Also note that article proofs via PDF do not show corrections that will have been made by the typesetter's proofreader, which generally include corrections of errors of page layout, figure placement, and spacing and font mistakes; feel free to mark any errors you notice in these areas. **When sending us your corrections, if you are writing them by hand, please print clearly. If sending a fax, please do not write too close to the margins of the page, as these are often cut off in fax transmissions. Finally, please note that a delayed, incomplete, or illegible response may delay the publication of your article while we contact you.**

Q2 au: ApJ follows American usage of " that " to introduce restrictive clauses and " which " for nonrestrictive.

Q3 au: that/which

Q4 au: that/which

Q5 au: that/which

Q6 au: added " the formula "; OK?

Q7 au: that/which

Q8 au: replaced " for " with " of "

Q9 au: that/which

Q10 au: added " the " after " following "

Q11 au: replaced " by " with " with "

Q12 au: that/which

Q13 au: inserted comma after " envelope "

Q14 au: deleted colon after " nuclei "

Q15 au: Does " G " stand for " Gauss "?

Q16 au: added " the " after " during "

Q17 au: replaced " period " with " periods "

Q18 au: Column head OK for first column of Table 1? If not, please supply one.

Q19 that/which

Q20 au: that/which

Q21 au: changed date from 1999 to 2000 to match reference list

Q22 au: Can you provide an update?

Q23 au: Please check this reference; we can find no such article in ADS.

Q24 au: updated reference
Q25 au: Cannot find this reference in NASA ADS; I did find " Gaisser & Grillo 1987, Phys. Rev. D, 36, 2752 "; could this be it?
Q26 au: Please check this reference; we can find no such article in ADS.
Q27 au: Please check this reference; we can find no such article in ADS.
Q28 au: Can you provide additional editors for this, or is Ruderman the sole author?